

Constrained geometric simulation of the nicotinic acetylcholine receptor

William J. Belfield^a, Daniel J. Cole^{a,b}, Ian L. Martin^c, Mike C. Payne^a, P.-L. Chau^{d,*}

^a Theory of Condensed Matter Group, Cavendish Laboratory, Department of Physics, University of Cambridge, Cambridge CB3 0HE, United Kingdom

^b Department of Chemistry, Yale University, New Haven, CT 06520-8107, United States

^c Department of Pharmacology, University of Alberta, Edmonton, Alberta, Canada

^d Bioinformatique Structurale, CNRS UMR 3528, Institut Pasteur, 75724 Paris, France



ARTICLE INFO

Article history:

Accepted 2 May 2014

Available online 6 June 2014

Keywords:

Nicotinic acetylcholine receptor

FRODA

FIRST

Membrane protein

Cys-loop receptors

Ligand-gated ion channels

ABSTRACT

Constrained geometric simulations have been performed for the recently published closed-channel state of the nicotinic acetylcholine receptor. These simulations support the theory that correlated motion in the flexible β -sheet structure of the extracellular domain helps to communicate a “conformational wave”, spreading from the acetylcholine binding pocket. Furthermore, we have identified key residues that act at the interface between subunits and between domains that could potentially facilitate rapid communication between the binding site and the transmembrane gate.

© 2014 Published by Elsevier Inc.

1. Introduction

The nicotinic acetylcholine receptor (nAChR) is the archetypal member of the cys-loop family of ligand gated ion channels. The structure of the receptor, from *Torpedo marmorata*, has been determined by cryoelectron microscopy to a resolution of 4 Å (PDB structure code: 2BG9). It is composed of five subunits, two α -subunits together with single copies of β , γ and δ , arranged pseudosymmetrically around the integral ion channel, which spans the cell membrane and is selective for cations [1]. Recent studies, subsequent to time limited exposure of this protein to the natural agonist, have furnished images of the open channel structure [2], providing a structural image at both the ground state and the activated state of this important oligomeric protein. The physiological relevance of this receptor has led to detailed study of the biophysical consequences of its activation [3]. Of particular value here is rate-equilibration free energy relationship (REFER) analysis that has supplied a time-sensitive trace exploring the movement of individual structural blocks within the protein during the activation process [4]: thus providing an opportunity to explore the detail of the structural change in this protein that occurs between cryoelectron microscopic images of the ground and activated states.

Despite these experimental studies, little is known at an atomistic level concerning the gating mechanism, namely the movements that occur following ACh binding that result in a widening of the transmembrane pore. In this respect, molecular dynamics (MD) is a valuable computational tool for investigating interactions and correlations in a structure at the level of individual atoms and residues. So far, the only MD simulation performed on the 2BG9 coordinates is that of Liu et al. [5]. In this work, the authors show that inward movement of the C-loop, at the ACh-binding pocket, causes rotational movement of the transmembrane helices around the pore axis. In addition, Gao et al. [6] performed simulations on the acetylcholine-binding protein (AChBP), Law et al. [7] used the AChBP crystal coordinates and the nAChR cryo-electron microscopy coordinates as templates to build a combined model of the ($\alpha 7$)₅-subtype of the nAChR, and Cheng et al. [8] created a different model of the ($\alpha 7$)₅-subtype of the nAChR, while subsequent work used principal component analysis to identify the movements responsible for gating [9]. Despite providing valuable information, all this work was carried out before the open-channel structure of the nAChR had been determined by experiment and so does not benefit from the additional information this structure contains.

Recently, Unwin and Fujiyoshi [2] proposed a gating mechanism for moving from the closed-channel form to the open-channel form based on their experimental structures. They suggest that binding of ACh causes an orthogonal displacement of β -sheets of the α_{γ} -subunit. This structural shift then induces a displacement of the

* Corresponding author. Tel.: +33 1 45688546; fax: +33 1 45688719.

E-mail address: pc104@pasteur.fr (P.-L. Chau).

β -subunit away from the pore axis, which, in turn, destabilises the pentameric arrangement of helices making up the central hydrophobic gate. This destabilisation permits the M2 helices of both the α_γ - and δ -subunits to adopt straighter conformations, thus widening the pore radius. In their model, the opening of the channel is asymmetric, starting with the α_γ -subunit, moving out to the β -subunit and then the other three subunits.

In order to investigate the gating mechanism of the nAChR in more atomistic detail, one could employ MD simulations coupled with artificial forces to bias the trajectory [10,11] between the open and closed states. However, these methods are costly in computer time and require the application of arbitrary biasing forces which make it difficult to interpret the results quantitatively. In this work, we investigate the use of constrained geometric simulations, as implemented in the FRODA software [12], followed by cross-correlation analysis, principal component analysis and site-directed mutagenesis, to study the motion of the nAChR. In particular, we investigate how networks of constraints, identified by the FIRST software, lead to correlated motions in the protein that are consistent with, and hence support, the gating mechanism proposed by Unwin and Fujiyoshi [2].

2. Methods

FRODA is a protocol for performing geometrically constrained simulations of proteins. It is a computationally inexpensive method for sampling protein conformational space. Rather than the Newtonian dynamical approach of MD simulations, it employs a Lagrangian constraints-based approach, outputting an ensemble of structures that obey pre-defined constraints on bond lengths and angles, hydrogen bonds and hydrophobic interactions. Introducing such constraints allows efficient sampling of a relevant subspace of the total conformational search space, at the cost of being limited to a fixed constraints topology and generating an athermal ensemble. Explicit electrostatic interactions are not included in the computational model, and the effect of the solvent is included only indirectly by identifying and constraining hydrophobic interactions in the protein. FRODA has been widely used, for example, in studying the impact of intracellular flexibility upon the conductance of the 5-HT₃ ion channel [13], the effects of correlated motion on the transport of electronic excitations through photosynthetic bacteria complexes [14], protein–protein docking involving multiple conformational changes [15], elucidating cisplatin cross-linking in calmodulin [16], and monitoring flexibility of myosin during the ATPase cycle [17]. In comparative tests, fluctuations in an ensemble of FRODA-generated HIV-1 transactivation responsive region RNA structures agreed well with MD and NMR fluctuations [18] and FRODA outperformed MD in sampling transient pockets at protein–protein interfaces [19], indicating that dynamics of the native state emerge naturally from a simple network of native contacts.

FRODA simulations were performed with the FIRST/FRODA version 6.2 software downloaded from <http://flexweb.asu.edu/>. Full details of the method may be found elsewhere [12,20]. FRODA takes, as an input, a decomposition of the protein into rigid and flexible regions provided by the FIRST software.

The starting structures for the simulations were those of Unwin and Fujiyoshi [2], in the open- and closed-channel states (4AQ9 and 4AQ5, respectively). The structures were protonated using the AMBER11 package [21]. The default protonation state of titratable residues at pH 7 was used, and the resulting structures were checked by eye. The membrane was not added to the computational model, though, as we shall show later, the transmembrane domain comprises a series of large rigid clusters that are expected to be unaffected by this approximation. Missing residues in the β -loops of subunits β , δ and γ were not included, because they

are expected to be flexible, and are distant from our main sites of study (the α_γ subunit and its interface with β). Suitable structures for input to FIRST were generated via 250 steps of steepest descent minimisation followed by 250 steps of conjugate gradient minimisation, both in the gas phase using the AMBER11 package [21]. To generate rigid cluster decompositions, the hydrogen bond energy cut off (E_{cut}) was set to -4.2 kJ/mol. The principal component subspaces spanned by FRODA simulations have been shown to be very robust with respect to the chosen value of E_{cut} [22].

For FRODA dynamics, a step length of 0.1 \AA [22] was employed. Sixteen simulations, each sampling 275,000 configurations, were run starting from the open-channel structure, and sixteen were run starting from the closed-channel structure. For each state, the sixteen simulations started from the same structure, but used a different random seed for the atomic moves, thus ensuring independent trajectories. Our results for the open-channel structure are qualitatively similar to those of the closed-channel structure, and so, for simplicity, we focus exclusively on the closed-channel form in what follows. A total of 17,600 configurations were stored for analysis. The stereochemical quality of the snapshots was ascertained via PROCHECK [23] – for all snapshots, the maximum number of bad contacts was 23 and fewer than 2.5% of the amino acids were in disallowed regions of the Ramachandran plot. The total computational time for all 16 runs was 1650 h on a single Intel Sandy Bridge core, which represents a substantial saving over typical MD simulations.

Root-mean-square fluctuations (RMSF) and cross-correlation analysis was performed on the C_α atoms of the stored configurations using the PTRAJ module of AMBER11 [21]. The cross-correlation coefficient C_{ij} between atoms i and j is defined as follows:

$$C_{ij} = \frac{\langle \Delta r_i \cdot \Delta r_j \rangle}{\sqrt{\langle (\Delta r_i \cdot \Delta r_i) \rangle \langle (\Delta r_j \cdot \Delta r_j) \rangle}} \quad (1)$$

where Δr_i is the displacement vector for atom i and angular brackets denote an average over the stored configurations. The resulting coefficient is a measure of the correlated nature of the motion of pairs of residues and ranges from -1 (anti-correlated) to $+1$ (correlated). This simple measure allows identification of long-range correlations that are not intuitive from the structure alone, and will be used in this study as a starting point for the identification of rigid clusters that may aid communication between the ACh binding site and the pore-lining helices. We note that recent improvements to the measurement of correlation coefficients, based on the calculation of mutual information, allow the identification of non-linear and non-colinear correlations that may be missed by Eq. (1) [24]. However, Eq. (1) has been shown to be accurate for the strongest correlations, and indeed we have confirmed that the pattern of correlations in the α_γ subunit is robust with respect to the correlation measure.

We have also performed a principal components analysis (PCA). PCA is a transformation generated by diagonalising the covariance matrix of the atomic fluctuations from their average positions, as generated from the ensemble of stored conformations. The elements of the covariance matrix are defined by:

$$\Gamma_{ij} = \langle (x_i(t) - \langle x_i(t) \rangle) \cdot (x_j(t) - \langle x_j(t) \rangle) \rangle \quad (2)$$

where $x_i(t)$ and $x_j(t)$ are the Cartesian coordinates for atoms i and j at time t , with the angle brackets indicating averaging over the ensemble. The new coordinate basis defined by the eigenvectors (arranged in descending order of eigenvalue) has the property that each eigenvector accounts for progressively less of the observed variance in the data.

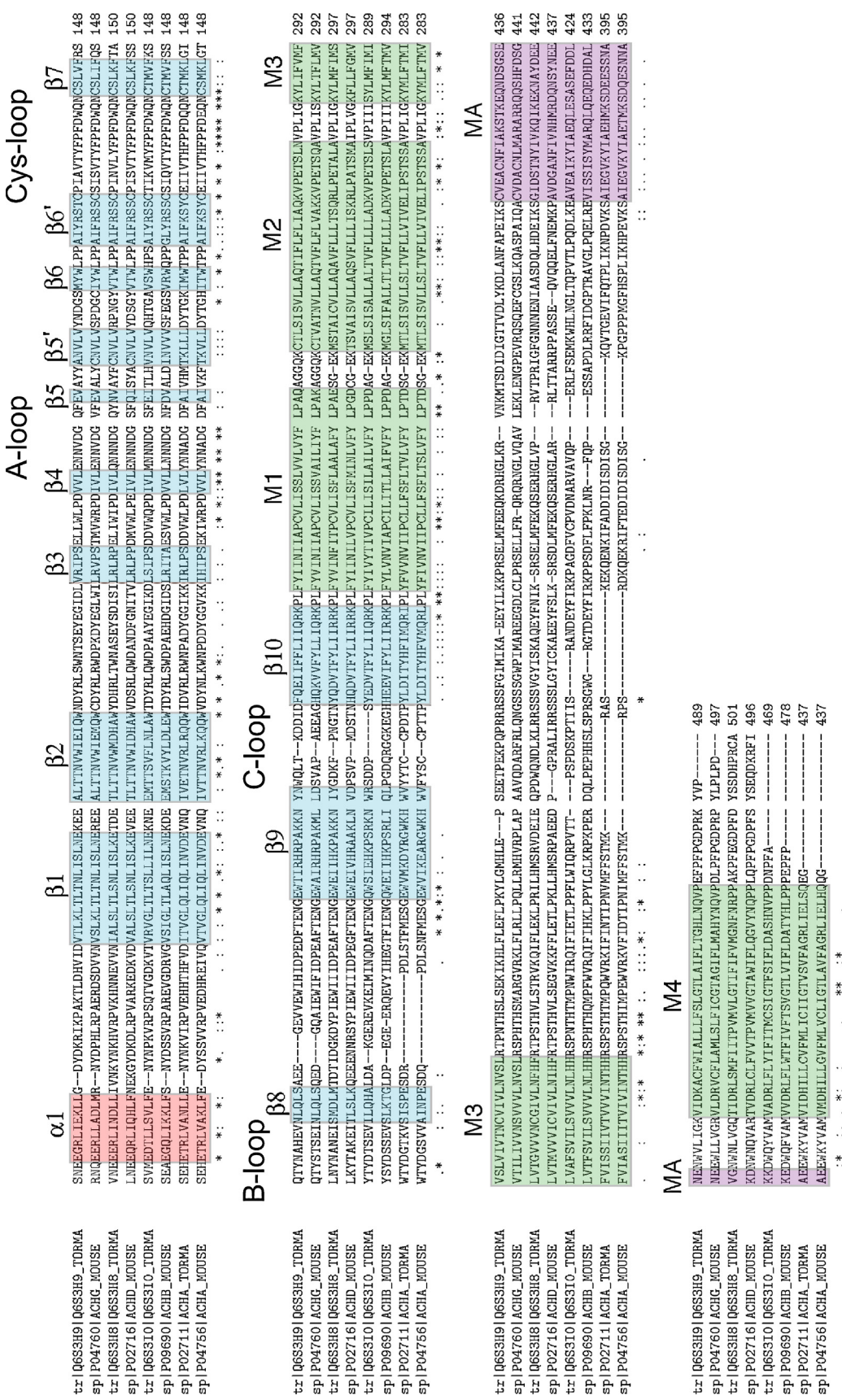


Fig. 1. The alignment of the nAChR sequences of *Torpedo marmorata* and *Mus musculus* (mouse). The *Torpedo* sequence numbers will be referred to in the subsequent diagrams. Secondary structure labelling is also indicated.

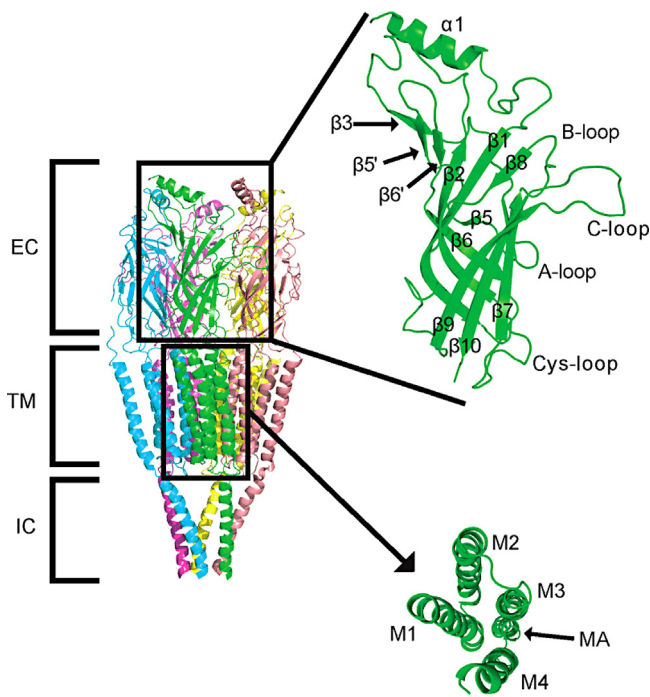


Fig. 2. The pentameric structure of the nAChR, with the insets showing the details of the extracellular domain, and the arrangement of the helices in the transmembrane domain.

3. Results

Fig. 1 shows the alignment of the nAChR sequences from *T. marmorata* and the mouse (*Mus musculus*), as well as the structural labels used in the text that follows. **Fig. 2** shows the pentameric structure of the nAChR, with the insets showing the details of the extracellular (EC) domain, and the arrangement of the helices in the transmembrane (TM) and intracellular (IC) domains. The EC domain comprises one helix and 12 β -sheets (**Fig. 1**). The ligand-binding

site is situated between the EC domains of two adjacent subunits. Viewed from the extracellular space, down the long axis of the pentamer, the subunit clockwise from the binding site is termed the subunit on the positive side, and the anti-clockwise subunit is on the negative side. Here, the positive subunit is an α -subunit, but the negative subunit is either the γ -subunit or the δ -subunit (**Fig. 3**). On the positive subunit the binding site is made up of the A-, B- and C-loops (**Fig. 1**), whilst on the negative subunit, the binding site is made up of the β_1 -, β_2 -, β_5 -, β_6 -strands and the β_8 - β_9 -linker [3]. The IC domain comprises the short loop between the M1 and M2 helices and the link between the M3 and M4 helices. However, electron microscopy could not resolve the structure of large stretches of this domain, except for the MA helix. Secondary structure prediction from the sequence suggests that the unresolved parts could be unstructured [25].

The nAChR models used in this study comprise nearly 30,000 atoms. In order to reduce the number of degrees of freedom to be explored computationally, we have used the FIRST software to decompose the structure into a series of rigid and flexible units based on identified covalent bonds, hydrogen bonds and hydrophobic tethers. **Fig. 3** shows the assignment of rigid units by FIRST for the closed channel form of nAChR (PDB code: 4AQ5). The largest rigid units are α -helices found in the TM and IC domains. Interestingly, the M2 helices separate into two distinct clusters, with a short section at the extracellular end, neighbouring a longer section on the intracellular side (**Fig. 3**, the helix in the middle of the diagram separates into a bright green and a blue section). Although there are several small rigid clusters, FIRST reveals that most of the flexibility in the nAChR protein is in the EC domains.

To elucidate how the static FIRST results translate into allowed structural dynamics, we have used the FRODA software to explore the conformational space of the closed channel form of nAChR. From sixteen independent trajectories, we have analysed the root-mean-square (RMS) fluctuations of each residue, constructed cross-correlation matrices and decomposed the motion into principal components, in order to explore the coupling between different regions of the protein.

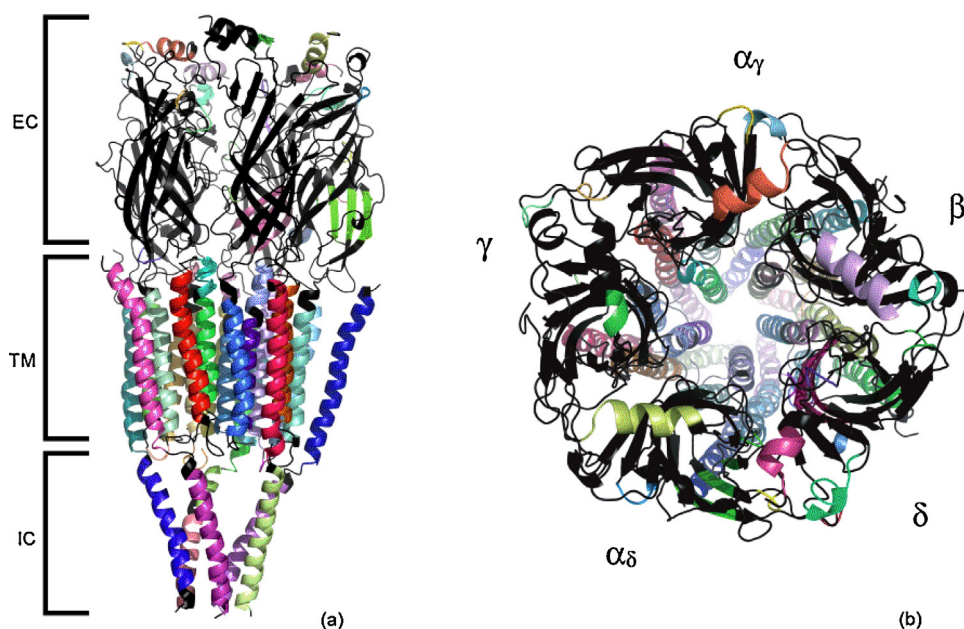


Fig. 3. FIRST assignment of rigid units. Different colours denote different parts of the protein which are considered rigid, while the parts of the protein which are coloured black are considered more flexible. (a) Side view of the nAChR. (b) View of nAChR from the extracellular space towards the intracellular space. The two binding sites are formed, respectively, by the α_γ - and γ -subunits, and the α_δ - and δ -subunits.

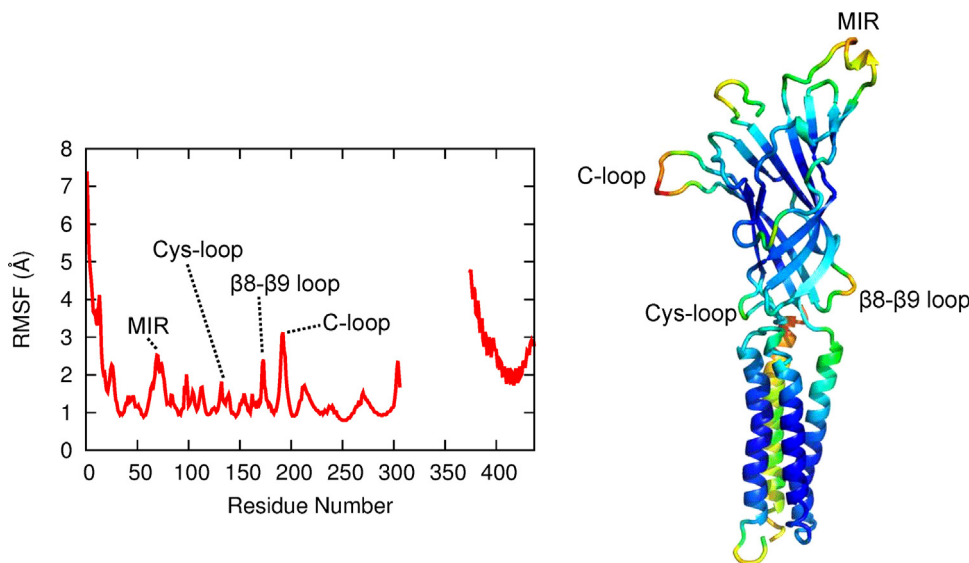


Fig. 4. (Left) RMSFs for the α_γ subunit. (Right) Colour-coded B-factors for α_γ residues 20–306.

3.1. Root-mean-square fluctuations

Fig. 4 shows the RMS fluctuations of residues of the α_γ subunit over the course of the FRODA simulations. Reasonably similar behaviour is observed in the other subunits – the main difference being that the β - and γ -subunits have very large fluctuations in the $\beta 8\beta 9$ loop due to missing residues in these subunits. Some similarities and some differences are observed between the current results and two sets of molecular dynamics simulations run on homology models of the nAChR structure [7,26]. The regions found to fluctuate most during the FRODA simulations were the N-terminus and intracellular end of the MA helix, the latter possibly being exaggerated by the absence of the intracellular loop connecting it to M3. Among the most mobile parts of the EC domain are the C-loop, MIR (main immunogenic region located in the $\beta 2\beta 3$ -loop) and $\beta 8\beta 9$ -loop. This is in good agreement with the MD results, although in the MD simulations the $\beta 8\beta 9$ -loop fluctuations are slightly larger than the C-loop, which could be a consequence of the model building process, where loops from the AChBP were used. Other mobile regions in the EC domain are the $\beta 1\beta 2$ -loop and Cys-loop, which are relatively close to the TM domain. On the TM side of the interface, a larger departure from the MD results is found, with the M2–M3 linker and pre-M1 linker undergoing significantly larger fluctuations in the MD simulations. Nevertheless, the consistency between the MD and FRODA simulations indicates that the current, computationally inexpensive representation of the system, lacking explicit solvation, membrane and ions, provides a reasonable picture of the flexibility of the studied system.

3.2. Communication between the binding site and transmembrane domain

The nAChR protein is activated by two ACh molecules binding to the two binding sites, respectively, at the α_γ - γ interface, and the α_δ - δ interface. ACh binds to the extracellular domains of these interfaces, whereas the ion channel gate is located in the transmembrane domain. Thus two processes have to take place to cause ion-channel opening: the propagation of changes from the binding sites ‘laterally’ to other subunits, and the propagation of changes from the extracellular domain to the transmembrane domain. Following the argument of Unwin and Fujiyoshi [2] that the α_γ subunit plays the primary role in propagating lateral communication and

that the β subunit plays the primary role in coupling these changes to the membrane, we focus our analysis on these two subunits.

3.2.1. Lateral propagation of motion

A central question in the gating mechanism proposed by Unwin and Fujiyoshi [2] concerns how structural changes induced by ACh binding at the α_γ - γ subunit interface propagate to the β subunit. Fig. 5 shows cross-correlations between residues of the α_γ EC domain. Loops B (residues 149–155) and C (residues 188–198) of the α_γ subunit have been shown to be key to acetylcholine binding; loop B contains the ACh-binding residue W 149, while loop C is thought to undergo the largest conformational change [2,6,27]. Interestingly, the motions of these two loop regions in our FRODA simulations are strongly correlated with clusters of residues spread throughout the α_γ EC domain; both loops are coupled with regions around the $\beta 1$ -strand (residues 28–44), the $\beta 2$ -strand (residues 49–60), the $\beta 3$ -strand (residues 78–81), the $\beta 6'$ strand (residues 121–127) and the $\beta 5'$ -strand (residues 107–110).

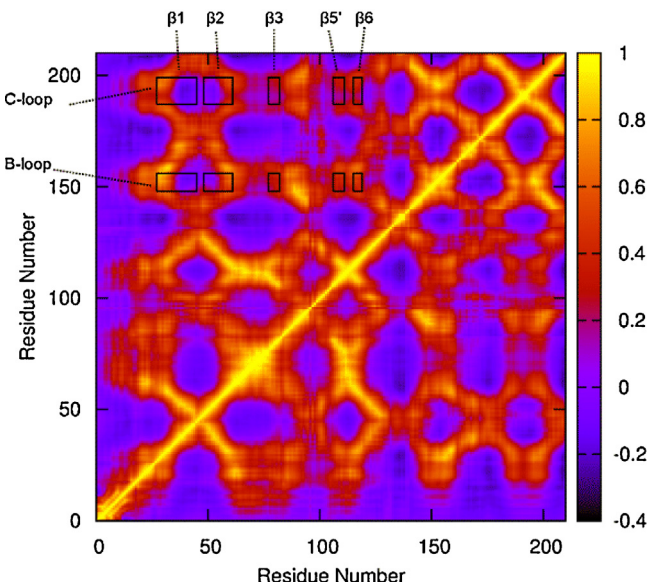


Fig. 5. Correlation between the movements of the amino acids of the α_γ -subunit EC domain. The key on the right shows the strength of the correlation.

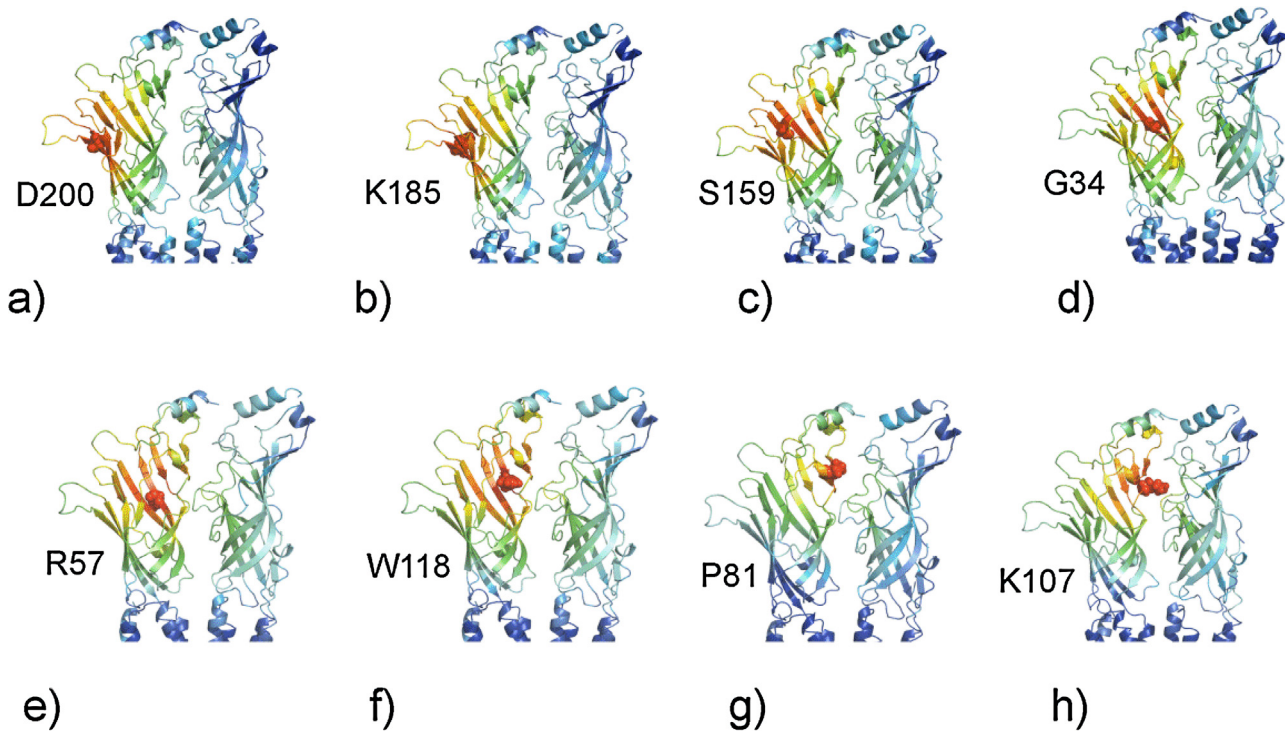


Fig. 6. A view of the α_γ - and β -subunits, looking from the central axis of the pentamer radially outwards. This diagram shows eight amino acids and their respective correlations with other parts of the α_γ - and β -subunits. Residues showing strong correlations in Fig. 5 were chosen to illustrate the proposed communication from the ACh binding site to the α_γ - β interface. The amino acid is shown in space-filling model, and the rest of the subunit is coloured according to the strength of the correlation, with red being a correlation of 1.0 and blue being a correlation of -0.3.

To further illustrate the proposed path of communication between the α_γ - γ interface and the β subunit, Fig. 6 shows the inter-residue correlations for a series of residues in the EC domain of α_γ . Panels (a-c) show how motions of residues Asp 200, Lys 185 and Ser 159, on respectively, the $\beta9$ -, $\beta10$ - and $\beta8$ -strands (strands flanking the C- and B-loops) are correlated to motions of the other residues in the α_γ - and β -subunits. Panels (d-f) show the correlations for residues from the $\beta1$ -strand (Gly 34), $\beta2$ -strand (Arg 57) and the $\beta6$ -strand (Trp 118), respectively. Panels (g and h) show the correlation for, respectively, residue Pro 81 on the $\beta3$ -strand, and Lys 107 on the $\beta5'$ -strand, which make contact with the β -subunit. This is a progression away from the binding site across the strands comprising the inner sheet and indicates the likely communication mechanism with the β -subunit.

To further support the hypothesis of a “conformational wave” emanating from the binding site, we have performed a PCA of the EC domain of the α_γ subunit. PCA of the ensemble of structures output from the FRODA simulation allows analysis of the dynamics in terms of its low frequency modes and aids visualisation of large-amplitude concerted motions. Fig. 7 shows the lowest frequency principal component (which accounts for approximately 20% of the overall fluctuations in the subunit). In agreement with MD studies of the nAChR, the C-loop of the α_γ subunit undergoes a relatively large amplitude swing motion towards the B-loop [9]. The C-loop closure is accompanied by a concerted shift of the β -strands in the direction of the β -subunit, which is consistent with their proposed role in inter-subunit communication. Further large amplitude motions are seen in the Cys- and $\beta1\beta2$ -loops.

3.2.2. α_γ - β subunit interface

Fig. 8 shows cross-correlations between residues of the α_γ and β extra-cellular domains. Interestingly, despite being separated by a distance of approximately 20 Å, there are evident couplings between residues of the α_γ B- and C-loops and specific motifs

within the β subunit. These couplings are mediated by the inner sheet strands described above. The strongest couplings are between the $\beta2$, $\beta3$, $\beta5'$ and $\beta6'$ strands on α_γ and the A-, B- and C-loops on the β -subunit. Fig. 8 reveals the possible atomistic mechanism by which correlation is communicated across the interface. FIRST

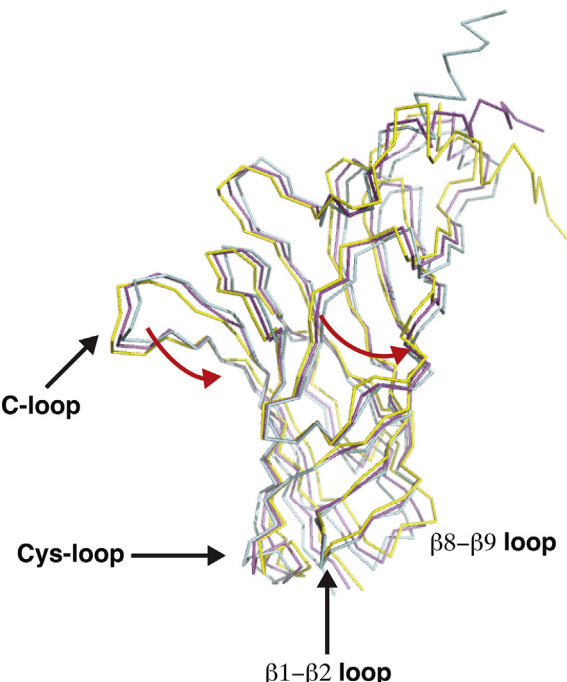


Fig. 7. The lowest frequency principal component for the C_α atoms of the α_γ subunit of nAChR. C-loop closure (yellow to magenta to cyan, movement out of the page) is associated with concerted motion of the EC β -strands in the direction of the β -subunit (red arrows).

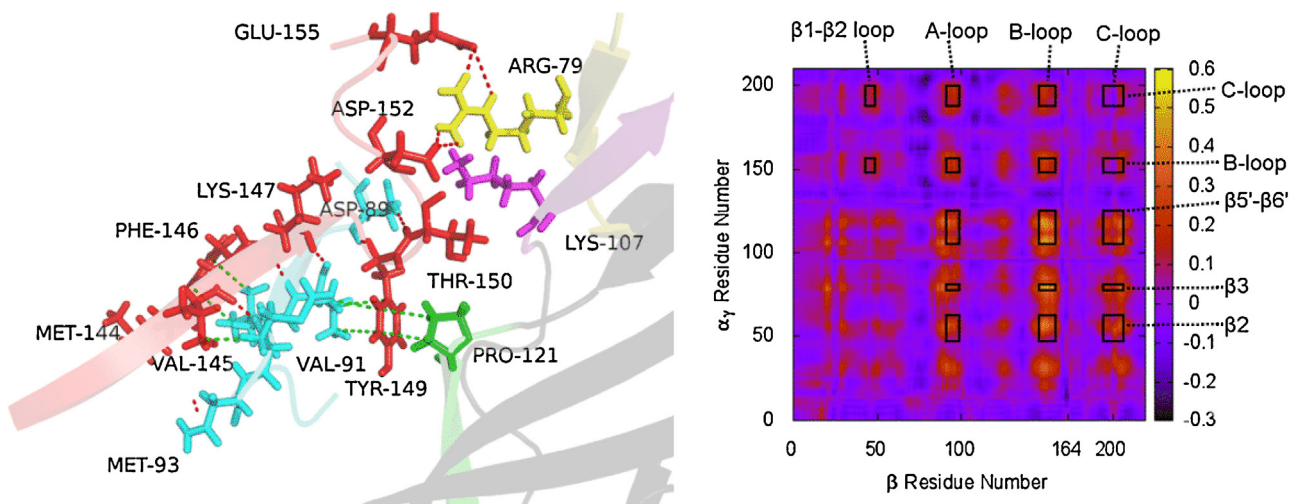


Fig. 8. (Left) Detailed view of the α_γ - β EC interface. Residues on the β subunit are coloured red and blue, while all other residues are on α_γ . Red dashed lines denote hydrogen bonds, and green lines denote hydrophobic tethers. (Right) Cross-correlation matrix between residues of the α_γ and β EC domains.

actually assigns Pro 121 on the α_γ $\beta 6'$ -strand and Tyr 149 on the β subunit's B-loop to the same rigid unit, since they are linked by a strong hydrophobic tether. The same is true of the Arg 79-Asp 152 and Arg 79-Glu 155 inter-subunit salt bridges between the α_γ , $\beta 3$ -strand and the β subunit's B-loop. The β -subunit A loop is not in direct contact with α_γ , but is tightly coupled to it via a hydrophobic interaction between Val 91 and Tyr 149, and hydrogen bonds linking Asp 89 with Tyr 149 and Thr 150. The β -subunit C-loop is coupled to the $\beta 2$ -strand of the α_γ by a salt bridge between Asp 192 and Arg 55.

One of the main advantages of the computationally-efficient constraints-based simulation of ion channel proteins, that is employed here, is that hypotheses concerning the gating process may be tested via site-directed mutagenesis of key residues. Following our observations that Tyr 149 appears to mediate communication between α_γ and the A-loop of the β subunit, we have performed a Y149A mutation (on the β subunit), thus removing the hydrophobic constraints involving Tyr 149 that are shown in Fig. 8. After running a FRODA simulation of the new structure under otherwise identical conditions, we have re-analysed the cross-correlations between residues of the α_γ and β extra-cellular domains. Fig. 9 reveals the difference in observed correlations between the two simulations. The main effect of the mutation is to decrease inter-subunit correlations, in particular, between the $\beta 2$, $\beta 3$, $\beta 5'$ and $\beta 6'$ strands on α_γ and the A- and B-loops on the β -subunit, as expected. We note that the correlations do not fall to zero, presumably due to the other interactions that span the interface. Nevertheless, we suggest that further investigation of the Y149 interactions using more accurate methods, or experiment, may help to further elucidate the gating mechanism in the nAChR.

3.2.3. Vertical propagation of correlation

If the β -subunit is to initiate gating, then we hypothesise that there must be communication from the extra-cellular to the trans-membrane domains of this subunit. Fig. 10 identifies four structural regions of the β -subunit that may be responsible for propagating this motion. The $\beta 1\beta 2$ - and A-loops were identified in the previous subsection as communicating with the α_γ -subunit. Here, they are also shown to be linked with movement in the β subunit TM domain, in particular the M1 helix (residues 213–224) and the M2–M3 linker (residues 264–296). More significantly, Fig. 8 reveals that Val 145 forms part of the same hydrophobic cluster as Val 91 and Tyr 149 on β and Pro 121 on α_γ , thus suggesting a mechanism for communication between α_γ and the Cys-loop (residues

131–138). In turn, the Cys-loop, along with the $\beta 8\beta 9$ -loop, appear to be the primary contributors to communication with the TM domain (Fig. 10). The two loops are strongly correlated with the M4 TM helix (residues 443–464), as well as the M1 helix and M2–M3 linker discussed above.

Fig. 11 shows non-covalent bonds, identified by FIRST, between residues of the EC and TM domains for the β -subunit that may play a role in communication across the interface. The signature Cys-loop notably forms several interactions with Tyr 283 (Phe 137 and Phe 135 form hydrophobic tethers and Phe 135 also makes a hydrogen bond). Tyr 134 interacts with both the pre-M1 and M2–M3 linkers, forming a hydrogen bond and hydrophobic tether with Arg 215 and a hydrophobic interaction with Ile 279. Other interactions with the TM domain are formed by the $\beta 8\beta 9$ - and $\beta 1\beta 2$ -loops. Multiple hydrophobic tethers are identified from the $\beta 1\beta 2$ -loop to the M2–M3 linker. Tethers are formed by Lys 46 to Pro 278 and Glu 45 to Val 277 and Ile 279. In addition, Glu 45 makes a salt bridge with Arg 206 in the pre-M1 linker. For the $\beta 8\beta 9$ -loop, the interactions consist of a hydrogen bond between Trp 186 and Lys 216, along with the hydrophobic tethers Trp 186 to Arg 206 and Gln 185 to Phe 219.

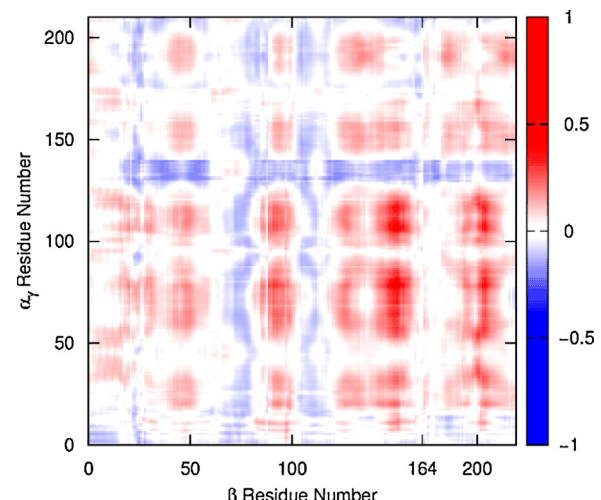


Fig. 9. Differences in cross-correlations between residues of the α_γ and β EC domains in the wild type and Y149A mutant nAChR. Red denotes a decrease in correlation upon mutation of Tyr 149 on the β subunit.

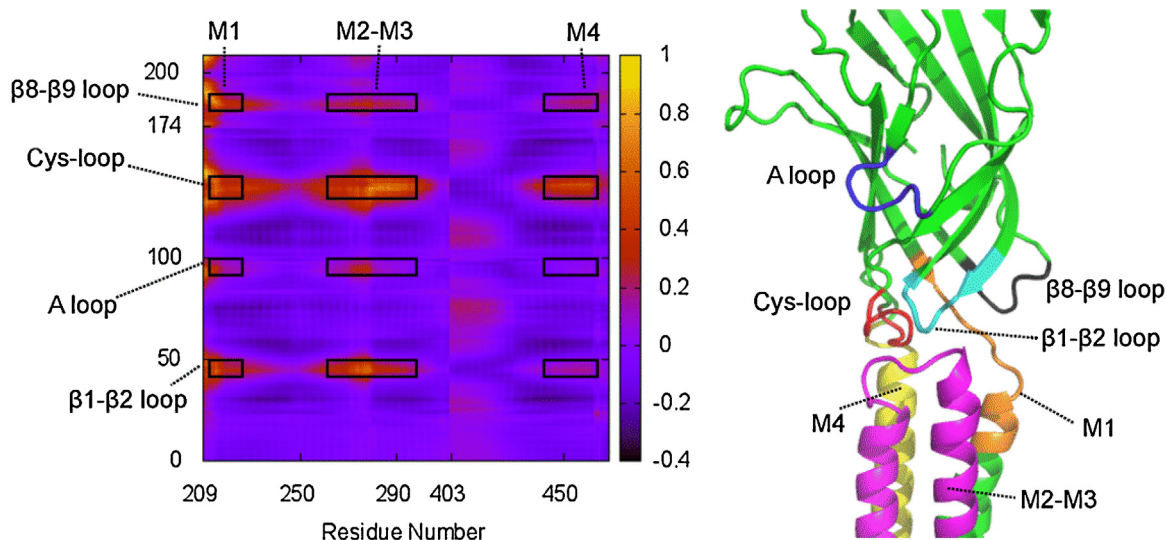


Fig. 10. β - β EC-TMD correlation. The left panel shows the cross-correlation matrix of the nAChR β -subunit, and the right panel shows the corresponding regions of the subunit structure. The cross-correlations between the extracellular domain and the transmembrane domain are annotated.

4. Discussion and conclusions

The nicotinic acetylcholine receptor is a protein responsible for initiating muscle contraction. It consists of five distinct subunits, placed pseudo-symmetrically around the central ion channel, within the post-synaptic membrane at the neuromuscular junction. On binding of two ACh molecules, its central ion channel switches open, via the gating process, thus initiating muscle contraction. Mutations of the nAChR can cause changes in its gating, which underlie a number of debilitating diseases [28,29], so a better understanding of this process is not only interesting scientifically, but also clinically important.

It is difficult to obtain large quantities of mammalian nAChR for structural studies. A structurally similar protein is the nAChR derived from the electric organ of the fish *Torpedo*. Its closed-channel structure has been determined by cryo-electron microscopy down to a resolution of 4 Å [1], and the coordinates of its open-channel form have recently been released [2]. In the proposed scheme, the two α -subunits are structurally different from the other three subunits, and are under structural strain. When acetylcholine binds to the nAChR, the strain is released first in the α_{γ} -subunit and then in the α_{δ} -subunit, and the central ion channel opens by a mixture of rotation and translation of the transmembrane helices. This work is a formidable experiment in electron microscopy, but the results do not provide us with the detailed atomistic dynamics, only the beginning and end points.

In order to explore the dynamics of the nAChR gating mechanism, we have employed constrained geometric dynamics, within the FIRST and FRODA software packages. Initial rigidity analysis was performed using FIRST, which revealed a more flexible EC domain and larger rigid clusters spanning the TM region. Interestingly, closer inspection of the M2 helices, revealed that they are separated into distinct rigid units, which could allow them to move independently. This observation is supported by results of rate-equilibration free energy relationship (REFER) analysis [30], which identifies residues towards the EC side of the M2 helices as moving earlier during the gating process than those on the IC side (for example, Φ -values range from 0.97 for Ser 268 to 0.26 for Leu 251) [31,32]. The concordance of these results go some way towards justifying our choice of hydrogen bond cut-off energy E_{cut} .

FRODA is a widely used technique for sampling allowed protein conformational space [15,17,18,13,16]. Using the FIRST rigidity analysis of the 4AQ5 structure as input, we have generated an

ensemble of closed channel forms. It is important to emphasise that we have not attempted to model the opening/closing process in its entirety. Such a study is precluded by the approximations made within FRODA (that are necessary for its computational efficiency) – no breaking or forming of constraints is allowed during unbiased dynamics, which may be required to transition from the closed to the open form. Furthermore, we have not considered the possibility that coupling between the C-loop of the α_{γ} subunit and the TM domain may be mediated by two or more orthogonal conformational transitions, as indeed proposed by Calimet et al. [33] in their description of the homomeric eukaryotic glutamate-gated chloride channel (GluCl). Such a sequence of opening events would be captured by molecular dynamics studies, although the length and time scales involved would make the effort computationally expensive, if not unfeasible, for the nAChR. Nevertheless, the methods described in the current study do allow us to explore how rigidity networks in the closed channel form may promote correlated dynamics and allow ACh binding to trigger a fast opening response. The computational efficiency of the approach allows us to rapidly perform “computational experiments” that may suggest further investigation using more accurate, but expensive, computational or experimental approaches.

We have first justified our use of FRODA dynamics by comparing the analysis of fluctuations in structural motifs of nAChR with corresponding MD simulations of the closed channel form. The agreement between the two methods is good, especially in the functionally important C- and β 8 β 9-loops at the ACh-binding site and the β 1 β 2- and Cys-loops at the EC-TM interface.

We have gone on to explain how correlated motion in the EC domain may help to support the proposed gating mechanism of Unwin and Fujiyoshi [2], which was based on direct visualisation of the nAChR structure. According to Unwin and Fujiyoshi [2], ACh-induced C-loop closure in the α_{γ} subunit leads to orthogonal displacement of β 1-, β 2-, β 6- and β 5'-sheets, towards the β subunit. This so-called “conformational wave” is fully supported by the FRODA simulations, which have revealed substantial correlated and concerted motion of the B- and C-loops with the network of β -sheets (Fig. 5). Such correlated motion theoretically allows rapid communication between the binding site and the β subunit without the need for slow conformational rearrangements.

Unwin and Fujiyoshi [2] propose that the α_{γ} -subunit propagates the motion further by ‘pushing’ its inner sheets against the neighbouring β subunit’s EC domain. We have shown that

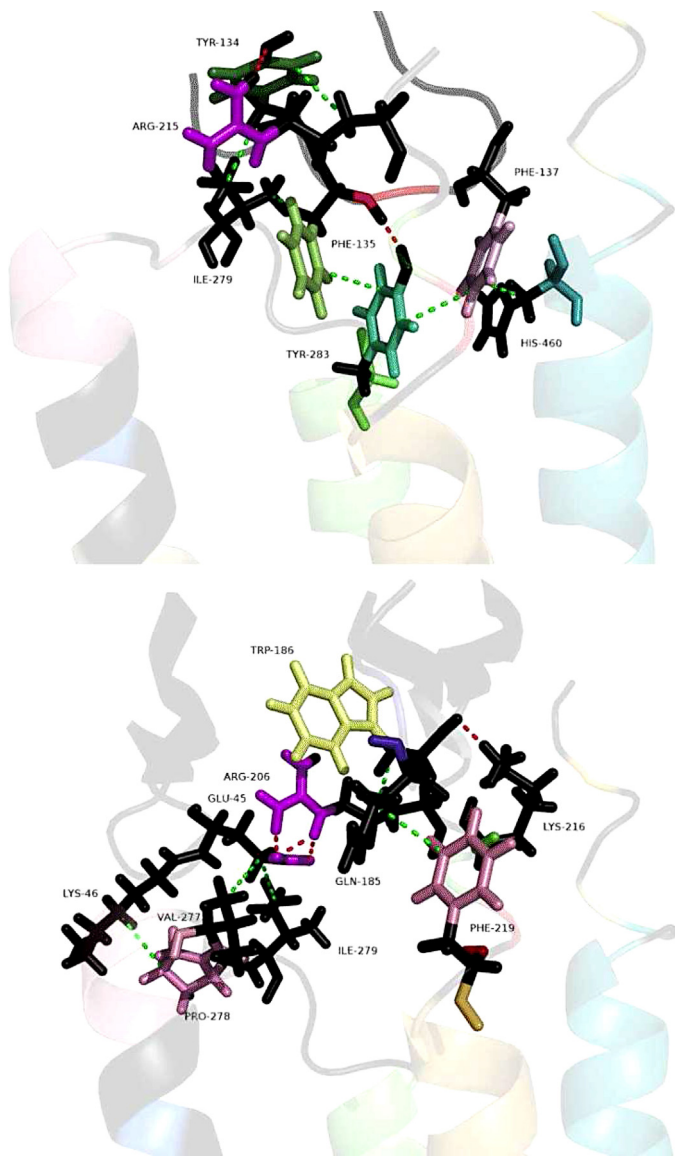


Fig. 11. Interactions between the EC and TM domains in the β -subunit. The interactions between the Cys-loop and the TM domain is shown on the top, and the other interactions are shown on the bottom. Atoms with the same colour are assigned to the same rigid unit by FIRST.

crucial interactions, in this respect, are formed by Tyr 149 on the B-loop of the β subunit, which couples with the $\beta\delta'$ -sheet on α_7 and the A-loop (also on the β subunit). We are not aware of any experimental mutagenesis studies of Tyr 149 on the β subunit, but we propose that loss of hydrophobic interactions at this interface would significantly decrease inter-subunit communication, potentially impacting the channel gating mechanism. This hypothesis is supported by the decrease in correlation between the α_7 and β subunits in FRODA simulations of the Y149A mutant, and the further observation that Tyr 149 is well-conserved across a wide range of species.

Finally, we have used our FRODA-generated conformational ensemble to investigate coupling across the EC-TM domain interface of the β subunit. This subunit was chosen due to the observation that β is the only subunit where displacement of the EC domain is tightly coupled to equal displacement of the membrane helices [2]. Again, Tyr 149 may be important in communicating motion to the Cys-loop of the β subunit (via Val 145). In addition, we have identified a number of interactions that span the domain

interface, thus correlating the response of the membrane helices with motion of the EC domain.

With the significant caveat that there is much ongoing debate over the relevance of homomeric prokaryotic receptors to the more complex members of the pentameric ligand-gated ion channel family [34], of which nAChR is one, we may compare our simulation data to the work of [33], which proposes a gating mechanism for GluCl. In that work, the same correlated motion between the $\beta 1$ - $\beta 2$ loop and the M2-M3 linker is observed that is shown in Fig. 10, and indeed, outer displacement of the latter is shown by Calimet et al. (2013) [33] to be further correlated with the ion pore radius. Furthermore, their observation of rigid body displacement of the beta sheets in the EC domain is echoed by correlations observed in the nAChR (see Fig. 6).

This work has shown the potential for using constrained geometric simulation methods in the investigation of complex movements of membrane ion-channel proteins. The identification, at low computational cost, of atomistic interactions that are capable of communicating large-scale correlated motions in proteins is expected to be a valuable tool to complement static crystal structure prediction.

Acknowledgements

The authors thank the UK EPSRC, the Canadian Institutes for Health Research (MOP 84286) and Queens' College, Cambridge, for support, Mizuki Morita, Anthony Auerbach, Grace Brannigan, Sakuraba Shun and Şebnem Essiz Gökhan for useful discussions, and Michael Rutter and Leung Hin-Tak for computing help. Computational resources were provided by the Cambridge HPC Service, funded by EPSRC Grant EP/J017639/1. DJC is supported by a Marie Curie International Outgoing Fellowship within the 7th European Community Framework Programme.

References

- [1] N. Unwin, Refined structure of the nicotinic acetylcholine receptor at 4 Å resolution, *J. Mol. Biol.* 346 (2005) 967–989.
- [2] N. Unwin, Y. Fujiyoshi, Gating movement of acetylcholine receptor caught by plunge-freezing, *J. Mol. Biol.* 422 (2012) 617–634.
- [3] S.M. Sine, End-plate acetylcholine receptor: structure, mechanism, pharmacology, and disease, *Physiol. Rev.* 92 (2012) 1189–1234.
- [4] S.V. Jadey, P. Purohit, I. Bruhova, T.M. Gregg, A. Auerbach, Design and control of acetylcholine receptor conformational change, *Proc. Natl. Acad. Sci. USA* 108 (2011) 4328–4333.
- [5] X. Liu, Y. Xu, H. Li, X. Wang, H. Jiang, F. Barrantes, Mechanics of channel gating of the nicotinic acetylcholine receptor, *PLoS Comput. Biol.* 4 (2008) e19.
- [6] F. Gao, N. Bren, T.P. Burghardt, S. Hansen, R.H. Henchman, P. Taylor, J.A. McCammon, S.M. Sine, Agonist-mediated conformational changes in acetylcholine-binding protein revealed by simulation and intrinsic tryptophan fluorescence, *J. Biol. Chem.* 280 (2005) 8443–8451.
- [7] R.J. Law, R.H. Henchman, J. McCammon, A gating mechanism proposed from a simulation of a human $\alpha 7$ nicotinic acetylcholine receptor, *Proc. Natl. Acad. Sci. USA* 102 (2005) 6813–6818.
- [8] X. Cheng, H. Wang, B. Grant, S.M. Sine, J.A. McCammon, Targeted molecular dynamics study of c-loop closure and channel gating in nicotinic receptors, *PLoS Comput. Biol.* 2 (2006) e134.
- [9] X. Cheng, I. Ivanov, H. Wang, S.M. Sine, J.A. McCammon, Barriers to ion translocation in cationic and anionic receptors from the Cys-loop family, *J. Am. Chem. Soc.* 129 (2007) 8217–8224.
- [10] J. Leech, J. Prins, J. Hermans, SMD: visual steering of molecular dynamics for protein design, *IEEE Comput. Sci. Eng.* 3 (1996) 38–45.
- [11] P.-L. Chau, Process and thermodynamics of ligand-receptor interaction studied using a novel simulation method, *Chem. Phys. Lett.* 334 (2001) 343–351.
- [12] S. Wells, S. Menor, B.M. Hespenheide, M.F. Thorpe, Constrained geometric simulation of diffusive motion in proteins, *Phys. Biol.* 2 (2005) S127–S136.
- [13] J.L. Kozuska, I.M. Paulsen, W.J. Belfield, I.L. Martin, D.J. Cole, A. Holt, S.M.J. Dunn, Impact of intracellular domain flexibility upon properties of activated human 5-HT3 receptors, *Br. J. Pharmacol.* 171 (2014) 1617–1628.
- [14] A.S. Fokas, D.J. Cole, A.W. Chin, 2014 (submitted for publication).
- [15] C.C. Jolley, S.A. Wells, B.M. Hespenheide, M.F. Thorpe, P. Fromme, Docking of photosystem I subunit Cusing a constrained geometric simulation, *J. Am. Chem. Soc.* 128 (2006) 8803–8812.

- [16] H. Li, S.A. Wells, J.E. Jimenez-Roldan, R.A. Romer, Y. Zhao, P.J. Sadler, P.B. O'Connor, Protein flexibility is key to cisplatin crosslinking in calmodulin, *Protein Sci.* 21 (2012) 1269–1279.
- [17] M. Sun, M.B. Rose, S.K. Ananthanarayanan, D.J. Jacobs, C.M. Yengo, Characterization of the pre-force-generation state in the actomyosin cross-bridge cycle, *Proc. Natl. Acad. Sci. USA* 105 (2008) 8631–8863.
- [18] S. Fulle, N.A. Christ, E. Kestner, H. Gohlke, HIV-1 TAR RNA spontaneously undergoes relevant apo-to-holo conformational transitions in molecular dynamics and constrained geometrical simulations, *J. Chem. Inform. Model.* 50 (2010) 1489–1501.
- [19] A. Metz, C. Pfleger, H. Kopitz, S. Pfeiffer-Marek, K.H. Barrington, H. Gohlke, Hot spots and transient pockets: predicting the determinants of small-molecule binding to a protein–protein interface, *J. Chem. Inform. Model.* 52 (2011) 120–133.
- [20] S.A. Wells, Geometric simulation of flexible motion in proteins, in: D.R. Livesay (Ed.), *Protein Dynamics*, vol. II, vol. 1084 of *Methods in Molecular Biology*, Humana Press, New York, 2013, pp. 173–192.
- [21] D.A. Case, T.A. Darden, T.E. Cheatham, C.L. Simmerling, J. Wang, R.E. Duke, R. Luo, R.C. Walker, W. Zhang, K.M. Merz, B. Robert, B. Wang, S. Hayik, A. Roitberg, G. Seabra, I. Kolossvary, K.F. Wong, F. Paesani, J. Vanicek, J. Liu, X. Wu, S.R. Brozell, T. Steinbrecher, H. Gohlke, Q. Cai, X. Ye, J. Wang, M.-J. Hsieh, G. Cui, D.R. Roe, D.H. Mathews, M.G. Seetin, C. Sagui, V. Babin, T. Luchko, S. Gusarov, A. Kovalenko, P.A. Kollman, AMBER 11, University of California, San Francisco, USA, 2010.
- [22] C.C. David, D.J. Jacobs, Characterizing protein motions from structure, *J. Mol. Graph. Model.* 31 (2011) 41–56.
- [23] R.A. Laskowski, M.W. MacArthur, D.S. Moss, J.M. Thornton, Procheck: a program to check the stereochemical quality of protein structure, *J. Appl. Crystallogr.* 26 (1993) 283–291.
- [24] O.F. Lange, H. Grubmüller, Generalized correlation for biomolecular dynamics, *Proteins* 62 (2006) 1053–1061.
- [25] V. Kukhtina, D. Kottwitz, H. Strauss, B. Heise, N. Chebotareva, V. Tsetlin, F. Hucho, Intracellular domain of nicotinic acetylcholine receptor: the importance of being unfolded, *J. Neurochem.* 97 (supp 1) (2006) 63–67.
- [26] X. Cheng, B. Lu, B. Grant, R.J. Law, J.A. McCammon, Channel opening motion of $\alpha 7$ nicotinic acetylcholine receptor as suggested by normal mode analysis, *J. Mol. Biol.* 355 (2006) 310–324.
- [27] R.H. Henchman, H.L. Wang, S.M. Sine, P. Taylor, J.A. McCammon, Asymmetric structural motions of the homomeric $\alpha 7$ nicotinic acetylcholine receptor as suggested by normal mode analysis, *J. Mol. Biol.* 355 (2003) 310–324.
- [28] O.K. Steinlein, D. Bertrand, Neuronal nicotinic acetylcholine receptors: from the genetic analysis to neurological diseases, *Biochem. Pharmacol.* 76 (2008) 1175–1183.
- [29] X.-M. Shen, J.M. Brengman, S. Edvardson, S.M. Sine, A.G. Engel, Highly fatal fast-channel syndrome caused by AChR ϵ -subunit mutation at the agonist binding site, *Neurology* 79 (2012) 449–454.
- [30] A.R. Fersht, R.J. Leatherbarrow, T.N.C. Wells, Quantitative analysis of structure–activity relationships in engineered proteins by linear free-energy relationships, *Nature* 322 (1986) 284–286.
- [31] A. Mitra, G.D. Cymes, A. Auerbach, Dynamics of the acetylcholine receptor pore at the gating transition state, in: *Proceedings of the National Academy of Sciences USA*, 2005, pp. 15069–21507.
- [32] P. Purohit, A. Mitra, A. Auerbach, A stepwise mechanism for acetylcholine receptor channel gating, *Nature* 446 (2007) 930–933.
- [33] N. Calinet, M. Simoes, J.-P. Changeux, M. Karplus, A. Taly, M. Cecchini, A gating mechanism of pentameric ligand-gated ion channels, *Proc. Natl. Acad. Sci. USA* 110 (2013) E3987–E3996.
- [34] G. Gonzalez-Gutierrez, C. Grosman, Bridging the gap between structural models of nicotinic receptor superfamily ion channels and their corresponding functional states, *J. Mol. Biol.* 403 (2010) 693–705.